International Journal of Microwave and Wireless Technologies, 2014, 6(3/4), 435–444.
doi:10.1017/S1759078714000282

RESEARCH PAPER

Classification of small UAVs and birds by micro-Doppler signatures

PAVLO MOLCHANOV[1], RONNY I.A. HARMANNY[2], JACO J.M. DE WIT[3], KAREN EGIAZARIAN[1] AND JAAKKO ASTOLA[1]

The popularity of small unmanned aerial vehicles (UAVs) is increasing. Therefore, the importance of security systems able to detect and classify them is increasing as well. In this paper, we propose a new approach for UAVs classification using continuous wave radar or high pulse repetition frequency (PRF) pulse radars. We consider all steps of processing required to make a decision out of the raw radar data. Before the classification, the micro-Doppler signature is filtered and aligned to compensate the Doppler shift caused by the target's body motion. Then, classification features are extracted from the micro-Doppler signature in order to represent information about class at a lower dimension space. Eigenpairs extracted from the correlation matrix of the signature are used as informative features for classification. The proposed approach is verified on real radar measurements collected with X-band radar. Planes, quadrocopter, helicopters, and stationary rotors as well as birds are considered for classification. Moreover, a possibility of distinguishing different number of rotors is considered. The obtained results show the effectiveness of the proposed approach. It provides the capability of correct classification with a probability of around 92%.

Keywords: Radar applications, Radar signal processing and system modeling

Received 15 October 2013; Revised 5 February 2014; first published online 19 March 2014

I. INTRODUCTION

Over the last years, the popularity of small unmanned aerial vehicles (UAVs) has boomed and is expected to increase even further [1]. Both in the military domain and in the civil domain mini-UAVs are more widely used, e.g. to obtain television footage of main events or to support first responders in dangerous areas. In particular, the civil market offers access to capable UAV technology for professionals and enthusiasts. On the Internet *do-it-yourself* components are readily available to build small fixed wing and rotary wing UAVs and the active community of enthusiasts pushes technology toward even more capable and scalable low-cost UAVs.

One concern of this increased popularity is violation of privacy when people operate mini-UAVs equipped with cameras. Another important concern is the abuse of mini-UAVs for protests, criminal acts or even terrorist attacks; in the wrong hands mini-UAVs may become arms or at least tools for harassment. For instance in May 2010 a mini-UAV was crashed into The Netherlands House of Parliament [2]. More recently, in September 2013, a small quadrocopter interrupted a meeting with the German Chancellor Merkel before crashing right in front of the lectern [3]. Although these incidents were probably more of a publicity stunt than anything else, they show that mini-UAVs pose an actual threat.

When considering mini-UAVs as a potential threat, suitable counteractions need to be developed. The first step in counteracting this threat is timely detection of incoming mini-UAVs. Small UAVs are however difficult to detect since they fly relatively slow and at low altitude (LSS-target). Moreover, flying birds may lead to (many) false alarms. Thus it is not only mandatory to timely detect incoming UAVs, but also to classify them as a suspect, potentially hazardous manmade target. Further classification into UAV classes, e.g. helicopter or multicopter, aids the threat assessment process.

Detection and classification of mini-UAVs can be performed with different types of sensors such as acoustic sensors, high-resolution infrared sensors and radar. In general detection by acoustic sensors is not very robust because mini-UAVs are relatively quiet and in the urban environment ambient noise levels may be high. High-resolution infrared sensors are capable of detecting mini-UAVs at practical distances and, after detection, they can zoom in on the target to obtain detailed imagery supporting classification. A drawback of infrared sensors is that they cannot provide speed and range of the target, and they are unsuitable for volume search and incapability to operate at fog and bad weather conditions. This is one of the strong points of radar, in addition to the ability to quickly scan a large volume. The focus of this study is therefore on radar detection and classification of small UAVs.

Some key radar techniques to classify airborne targets are high-range resolution profiling (HRRP), inverse synthetic

[1]Department of Signal Processing, Tampere University of Technology, Tampere, Finland
[2]Thales Nederland B.V., Delft, The Netherlands
[3]Department of Radar Technology, TNO, The Hague, The Netherlands
Corresponding author:
P. Molchanov
Email: pavlo.molchanov@tut.fi

aperture radar (ISAR) and analysis of micro-Doppler (m-D) signatures. The jet engine modulation (JEM) is a modulation of the radar echo signal from flying objects by rotating propellers of engines or compressor and turbine blades of jet engines [4]. We will refer to JEM in terms of m-D phenomenon. Classification on the basis of HRRP and ISAR relies on high resolution. To capture the spatial structure of mini-UAVs centimetre resolution is required. Consequently wide signal bandwidths are mandatory and in case of ISAR also long observation times with associated comprehensive motion compensation. HRRP and ISAR are demanding radar modes suitable for sophisticated radar systems (in terms of RF hardware and processing). With respect to analysis of m-D signatures, there is no need for high resolution or complex signal processing. Detection can be performed using moderate range resolution, i.e. of the order of decimeters, and afterwards detailed Doppler information can be obtained by operating the radar in continuous wave mode.

Over the years, m-D signatures have been used to classify humans, animals, and large (manned) aircraft [5]. Classification of mini-UAVs based on m-D signatures, on the other hand, is a novel topic. Nonetheless, m-D analysis shows potential not only to discriminate birds and UAVs, but also to separate different classes of UAVs, e.g. helicopters versus multicopters [6, 7].

Within this study, a complete chain for automatic target recognition (ATR) of UAVs based on m-D signatures has been developed. The successive steps in the ATR chain are: the generation of a spectrogram, noise reduction, alignment of the main Doppler component, feature extraction, and finally classification. New robust features are proposed that can be extracted from the aligned m-D signature. The proposed features are founded on basis functions of the m-D signature and they can be extracted by applying singular value decomposition (SVD) to the Doppler signature. The resulting features are orthogonal and unique providing essential and uncorrelated information about the target under consideration. The robustness of the novel features is assessed by feeding them to different types of classifiers. This assessment is performed using measured radar data of different types of targets such as fixed-wing UAVs, a quadrocopter, helicopters, rotating blades on a fixed position and birds. Each target type induces a unique m-D signature depending on the velocity and orientation of moving and rotating parts.

The main contributions of this study can be summarized as follows:

- A system for classification of UAVs by m-D signatures is developed;
- New robust features in the form of basis functions of the m-D signature are introduced;
- The performance of the ATR chain is assessed using measured radar data;
- The sensitivity of the classification performance to observation time, signal-to-noise ratio and rejection of the unknown target is assessed.

The rest of the paper is organized as follows. An overview of radar classification on the basis of m-D signatures is given in Section II. The proposed ATR chain is discussed in detail in Section III. The experimental verification is given in Section IV. Finally, conclusions are drawn in Section V.

II. THE M-D PHENOMENON

The m-D properties of a target are determined by moving and rotating parts in addition to the main body motion. The moving parts induce frequency and amplitude modulations on the backscattered radar wave. These modulations are unique for different types of targets since they depend on the specific configuration and rate of motion of the target's moving parts.

The different moving parts of a target act as separate scatterers, each inducing a distinctive Doppler frequency shift. The Doppler shift related to a single moving scatterer is given as:

$$f(n) = -\frac{2v(n)\cos\phi}{\lambda}, \tag{1}$$

where $v(n)$ is time-varying speed of a moving scatterer, ϕ is the angle between the velocity vector and the radar Line-of-Sight (LOS) and λ is the radar wavelength. The total signal received by the radar constitutes the contribution of all scatterers of a target:

$$s(n) = \sum_{k=1}^{K} a_k e^{j2\pi f_k(n)n/F_s} + \epsilon(n), \tag{2}$$

where K is the total number of moving scatters, a_k is the reflectivity of the k-th scatterer, $f_k(n)$ is the Doppler frequency shift of the k-th scatterer, $\varepsilon(n)$ is additive noise, F_S is a sampling frequency.

The Doppler information contained in (2) can be analyzed by computing the Doppler signature. On the basis of Doppler signatures it is feasible to estimate the main rotor configuration, rotor parity, tail rotor configuration, and hub configuration of (manned) helicopters [8]. Also, it has been demonstrated that turbojet aircraft, prop aircraft, and helicopters can be classified on the basis of jet engine modulation (JEM) characteristics.

If more detailed Doppler characteristics are required, e.g. to distinguish between different classes of mini-UAVs, it is common to analyze the time–frequency representation of (2), i.e. the so-called *spectrogram* [9]. The spectrogram can be obtained by applying successive, overlapping short-time Fourier transforms (STFT) to the time-domain signal (2). Also high-resolution transforms such as the Capon transform, Wigner–Ville distribution or Hilbert–Huang transform can be used.

An example of a spectrogram of a rotating helicopter blade is shown in Fig. 1. Two key positions of the helicopter blade with respect to the radar LOS are shown. In the position marked as "1" the blade is parallel to the radar LOS. The angle ϕ between the blade tip velocity vector v and the radar LOS is 90° resulting in near zero Doppler shift (note that the hub is stationary). In the position marked as "2" the blade is perpendicular to the radar LOS. In this case, the angle ϕ is 180° resulting in the maximum Doppler shift. Moreover, in position "2" the complete blade is observed by the radar inducing a flash in the spectrogram from zero velocity (i.e. the hub velocity) up to v (i.e. the blade tip velocity). From this simple example it is clear that different characteristics of a rotary-wing aircraft can be extracted from the spectrogram, e.g. the blade rotation rate can be determined by

https://doi.org/10.1017/S1759078714000282 Published online by Cambridge University Press

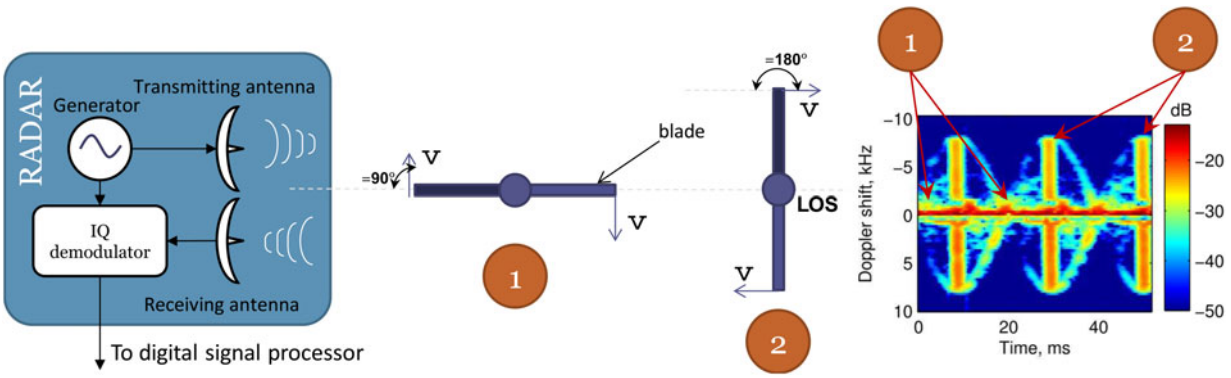

Fig. 1. Continuous wave radar and example of the spectrogram of m-D phenomenon from rotating propeller (top view).

counting the number of blade flashes per unit of time. In general, the spectrogram depends on the shape, tilt angle, blade length, number of blades, and blade rotation rate.

Indeed, by analyzing the spectrogram, the number of blades and rotation rate can be estimated [10] using varying techniques such as tomographic features [11] or maximum likelihood estimation of helicopter parameters [12]. These methods are able to distinguish different classes of UAVs, but they cannot separate different UAV models within a class. To separate different models within a class, more detailed information than just the number of blades and the rotation rate is needed.

Detailed information about the UAV parameters can be obtained by decomposition of the m-D signature. In [13], the wavelet transform is applied with time–frequency analysis for decomposition of the m-D signature. This study shows that after the signal decomposition the motion parameters of a helicopter can be estimated with higher precision. In [14] the Hilbert–Huang transform is used to obtain high resolution time–frequency information. In this study, the Hilbert–Huang transform is applied to the m-D signature of JEM decomposing the signature into separate signals. Above mentioned techniques could be used together with the proposed one to increase the performance.

III. PROPOSED APPROACH

A) General scheme

Scheme of the proposed classification system is illustrated in Fig. 2. The approach processes the radar signal sampled at two different sampling rates: 32 and 3.2 kHz to discriminate objects with wide (helicopters) and narrow (birds, planes) Doppler bandwidth. All information is contained in the branch of 32 kHz, however, to decrease the processing time we use a second sampling rate (3.2 kHz) with different parameters of feature extraction procedure. There is no practical need of the second ADC (3.2 kHz) as these information could be retrieved from the radar data sampled at 32 kHz followed by a down-sampler. Once the signal from radar is sampled, it passes through the m-D signature estimation, filtering, alignment, feature extraction, and classifier blocks, then the final decision (with confidence score) is made. Let us consider all of these blocks in detail.

B) Estimation of m-D signature

The m-D signature of the moving target is estimated as the magnitude of the spectrogram of the Doppler signal:

$$S(w,t)=\left|\sum_{m=0}^{M-1} W(m)s(m+(t-1)(M-L))e^{-j2\pi wm/M}\right|, \quad (3)$$

where $W(m)$ is the smoothing window function of length M, for instance, Hamming window can be used; w is the frequency index; L is the overlap of successive Fourier lengths, expressed in samples; the dimensionality of the spectrogram is $S\in\mathbb{R}^{M\times Q}$, $Q=\left\lfloor\frac{N-L}{M-L}\right\rfloor$; N is a total number of samples (length of s).

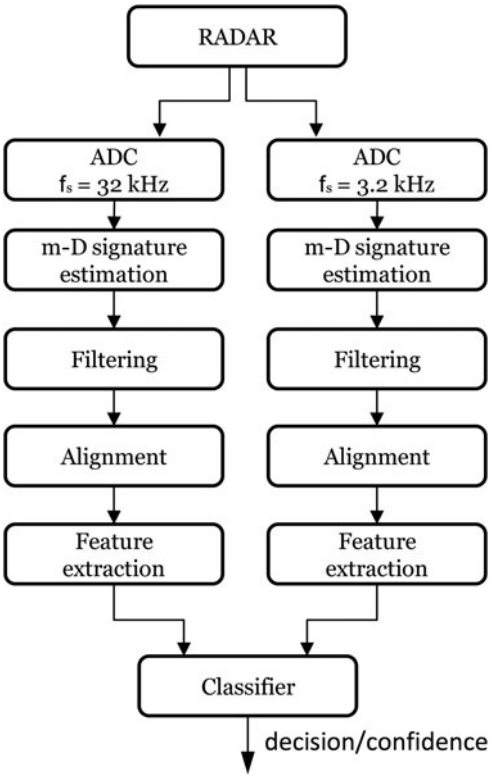

Fig. 2. Block scheme of the proposed approach.

https://doi.org/10.1017/S1759078714000282 Published online by Cambridge University Press

C) Filtering

The noise ϵ together with clutter could be removed from the observation s by the "spectral subtraction" noise reduction procedure [15]. The main idea of this approach is subtraction of an estimate of the average noise spectrum from the noisy signal spectrum. We assume that noise exhibits a static frequency profile with varied gain.

The average noise spectrum is estimated by a periodogram:

$$\Upsilon(w) = \frac{1}{Q}\sum_{t=1}^{Q} S^{(\epsilon)}(w, t), \tag{4}$$

where $S^{(\epsilon)}$ is STFT of noise only signal ϵ.

The gain of noise is estimated as a normalized length of the projection of the noisy signal spectrum onto noise spectrum:

$$G(t) = \sum_{w=1}^{M} \frac{\Upsilon(w)S(w, t)}{\|\Upsilon\|^2}, \tag{5}$$

where $\|\Upsilon\| = \sqrt{\Upsilon(1)^2 + \Upsilon(2)^2 + \ldots + \Upsilon(M)^2}$ is a Euclidean norm of the noise pattern.

The noise can be removed from the signature as:

$$U(w, t) = S(w, t) - G(t)\Upsilon(w). \tag{6}$$

In order to make U non-negative:

$$U(\cdot) = \begin{cases} U(\cdot), & \text{if } U(\cdot) \geq \beta S(\cdot) \\ \beta S(\cdot), & \text{if } U(\cdot) < \beta S(\cdot) \end{cases} \tag{7}$$

The threshold is set to be at level $\beta = 0.01$.

D) Alignment of the m-D signatures

In order to extract behavior of m-D features the motion of the target must be compensated. This can be done by tracking the change of velocity of the target's body.

Let us assume that the target's body is a scatterer with the highest reflectivity coefficient. Therefore, the target's body will appear as the maximum at the STFT. We need to track this maximum and then compensate the motion. However, the contribution of the stationary clutter is not removed yet. For this purpose, we propose to apply a weighting function before estimating the maximum:

$$h(w) = -\gamma e^{-\frac{w^2}{2\sigma^2}}, \tag{8}$$

where $\gamma = 128000/F_s$, $\sigma = 7\cdot(3200/F_s)^3$ and F_s is sampling frequency. It should be noticed that the weighting function h is obtained in dB scale. The parameters of the weighting function are selected empirically to maximize the classification rate on the training data. The weighting function assumes that stationary clutter contributes to near zero Doppler frequencies only, with stationary amplitude, estimated on signal-free data; therefore, it has a form of constant function with amplitude 0 dB and a gap of $-\gamma$ dB at zero Doppler.

As initial points to track the target's body motion, we take 10% of samples with the highest amplitude from the spectrogram. Then, unsupervised clustering is applied to reduce the number of initial points within the neighboring area. Then for each remaining initial point, the maximum is tracked within a local window with first increasing and then decreasing time index. In such a way, we obtain a number of possible tracks. Then the track corresponding to the maximum accumulated energy is selected as the target's body track $V(t)$.

The tracked velocity $V(t)$ is approximated by a polynomial of order 1 to reduce the number of outliers. In such a way the track is assumed to be a simple line, meaning that motion can contain only linear acceleration. The m-D signature is shifted then: $\hat{U}(w, t) = U(w + \hat{V}(t), t)$. The last procedure is done by linear interpolation. Empirically, we found that for a short observation time (decision making interval is 0.5 s) linear track is a reasonable choice for considered types of UAVs.

Finally, the m-D signature is ready for feature extraction.

E) Feature extraction

The features are based on extraction of bases of the m-D signature. These bases are orthogonal to each other and contain essential information about the rotating parts of the target. After the alignment, we assume that the spectrogram can be viewed as a low rank matrix.

First, we need to compute the correlation between different frequency components. Correlation matrix is computed as:

$$\Psi(w_1, w_2) = \sum_{t=1}^{Q} \hat{U}(w_1, t)\hat{U}(w_2, t). \tag{9}$$

Second step is to estimate eigenpairs $\{v_r, \lambda_r\}$, where v_r is r-th eigenvector and λ_r corresponds r-th eigenvalue, such that $\lambda_1 > \lambda_2 > \ldots \lambda_r$. Each eigenpair satisfies the following equality:

$$\Psi v_r = \lambda_r v_r. \tag{10}$$

Eigenvectors are orthogonal and unique forming the basis functions of the signal's spectrum. Eigendecomposition of Ψ or singular value decomposition of $\hat{U}$ can be used for estimation of eigenpairs. The steps (9) and (10) are similar to principal component analysis (PCA) with only small difference [16]. For PCA, the data must be mean centered before calculating the correlation matrix. In our case, the first (and the most important) eigenvector corresponds to the mean vector of the spectrogram.

Next, the Fourier transform of the eigenvectors is computed to obtain features with strong "energy compaction" property, i.e. the features where most of the signal information is concentrated. Typically, the signal information is contained in just a few low-frequency components. Owing to this property, we can calculate only the I first (low-frequency) coefficients to represent the data:

$$y_r = \bigcup_{l=1}^{I} \left\{ \left| \sum_{p=1}^{M} v_r(p) e^{-j2\pi pl/M} \right| \right\}. \tag{11}$$

Finally, the feature set is obtained by combining the first Z

https://doi.org/10.1017/S1759078714000282 Published online by Cambridge University Press

transformed eigenvectors and Z eigenvalues:

$$F = \bigcup_{r=1}^{Z} \{y_r, \lambda_r\}. \quad (12)$$

F) Classifier

In this paper, three different types of classifiers are considered in order to evaluate the robustness of the proposed features. The first two classifiers are the linear and non-linear support vector machines (SVMs) belonging to non-probabilistic classifiers, and the third one is the Naive Bayes classifier (NBC) belonging to probabilistic linear classifiers.

1) NAIVE BAYES CLASSIFIER

Naive Bayes classifier decides in favor of the class with the highest posterior probability, assuming that the features associated with each class are conditionally independent.

The decision is based on the maximum of class conditional probability:

$$\hat{C} = \max_C P(C|F), \quad (13)$$

where F is a feature vector.

Considering the Bayes' theorem and assuming the conditionally independent properties of features, the decision can be expressed as:

$$\hat{C} = \max_C P(C) \prod_{n=1}^{N} P(F_n|C), \quad (14)$$

where $P(C)$ is a prior probability of class C; $P(F_n|C)$ is the likelihood function; F_n is the feature n.

Commonly, the prior probability is unknown and the equation is solved by maximizing the product of likelihood functions. Therefore, the decision rule is called the maximum likelihood (ML). Finally, the ML rule can be written as:

$$\hat{C} = \max_C \prod_{n=1}^{N} P(F_n|C). \quad (15)$$

According to the method of estimating $P(F_n|C)$ the Naive Bayes classifier can be considered as normal or kernel-based. In the first case, the likelihood function is approximated from the Gaussian distribution. In the second case, the likelihood function is approximated by a kernel smoothing density function.

2) SUPPORT VECTOR MACHINE (SVM)

Support vector machines belong to the non-probabilistic kind of binary classifiers. In this paper, we use the version of a SVM with soft margins proposed in [17]. Assuming the linearly separable classes, a hyperplane with maximal margins can be found to separate the classes with minimum error. The SVM can be extended to the multiple hypothesis classifier combining various SVMs using the one-against-one approach.

Assuming the training set of instance-label pairs $R_i = \{F^{(i)}, c_i | F^{(i)} \in \mathrm{R}^n; c_i \in \{1, -1\}\}$ is given, the support vectors are found by the solution of the following optimization problem:

$$\min_{w,b,\epsilon} \frac{1}{2} w^T w + S \sum_{i=1}^{I} \epsilon_i \quad \text{subject to } c_i(w^T \phi(F^{(i)}) + b) \geq 1 - \epsilon_i, \; \epsilon_i \geq 0, \quad (16)$$

where ϵ_i is the degree of misclassification of the data $F^{(i)}$; w and b describe the separation hyperplane; S is the penalty parameter of the error term; $\phi(\cdot)$ is the function which maps the data F into a higher dimensional space.

Actually, the SVM is a linear classifier. However, not all data are linearly separable in the data space. Therefore, the function $\phi(\cdot)$ is used for data mapping into a high dimensional space, where data are linearly separable with the minimum error (soft margin).

In this paper, we use a radial basis function: $K(F^{(i)}, F^{(j)}) = \exp(-\gamma \|F^{(i)} - F^{(j)}\|^2)$, $\gamma > 0$. Thus, the function $\phi(\cdot)$ is selected to satisfy $K(F^{(i)}, F^{(j)}) = \phi(F^{(i)})^T \phi(F^{(j)})$.

A number of parameters are required to characterize the SVM classifier. The hyperplane that separates classes is described by a few support vectors (few feature vectors, $F^{(i)}$). These selected support vectors are based on the training set. The parameter γ of mapping function $\phi(\cdot)$, and the penalty parameter S are estimated using cross-validation procedure for the training set using grid search. The considered parameters of S are equal to $\{\exp(-5,\ldots,5)\}$, and γ are $\{1/2\exp(2\sigma) | \sigma \in \{-4,\ldots,4\}\}$. The parameters of the SVM are selected empirically to maximize the classification rate on the training data.

IV. CLASSIFICATION RESULTS

A) Data collection

The proposed ATR system is evaluated on real radar measurements. The radar data have been collected with a continuous-wave radar operating in X-band at radio frequency of 9.5 GHz. These radar measurements have been performed within the framework of D-RACE, the Dutch Radar Centre of Expertise, a strategic alliance of Thales Nederland B.V.

Table 1. UAVs used for experimental verification of the proposed ATR system. Type 'P' is for Plane, 'H' is for Helicopter, 'Q' for quadrocopter, 'B' for birds, 'S' for stationary rotors.

Class	Model	Type	# of rotors	Rotor, mm
1	YAK54 vliegtuig	P	1	100
2	EasyStar El-Sailor	P	1	108
3	Birds	B	–	–
4	Parrot AR.Drone	Q	4	200
5	1 rotor	S	1	203
6	2 rotor	S	2	203
7	3 rotor	S	3	203
8	4 rotor	S	4	203
9	Mikado Logo 600	H	2 (main, tail)	1350 (main)
10	Mikado Logo 400	H	2 (main, tail)	1040 (main)
11	Align T-REX 450	H	2 (main, tail)	715 (main)

https://doi.org/10.1017/S1759078714000282 Published online by Cambridge University Press

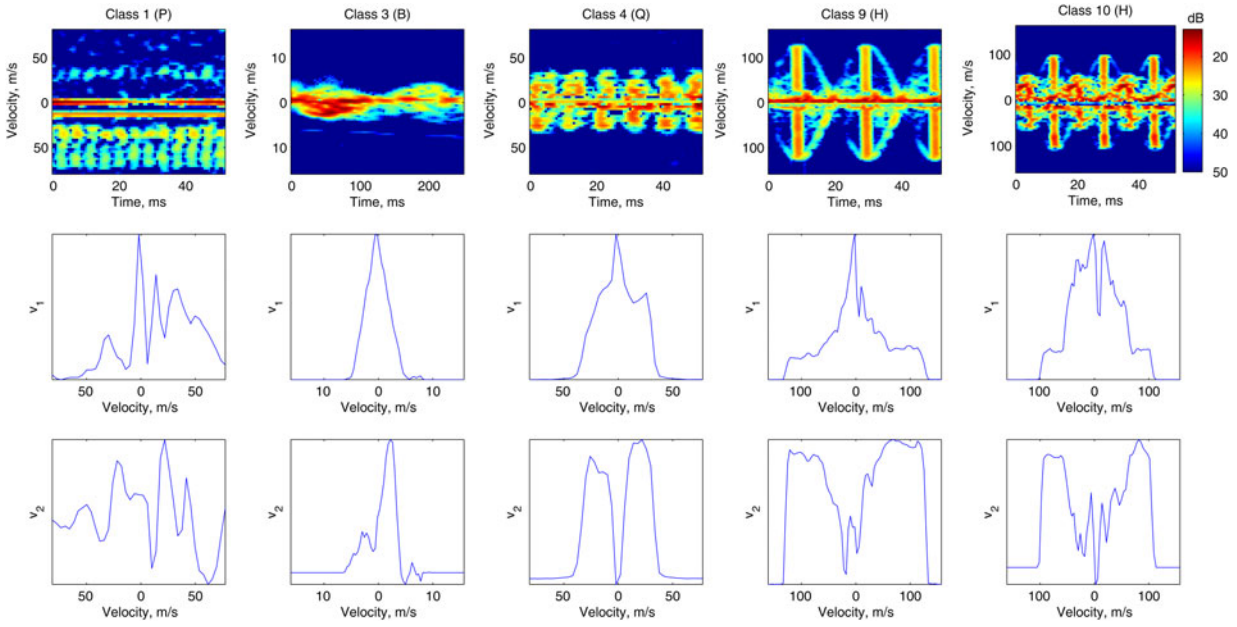

Fig. 3. Examples of filtered and aligned micro-Doppler (m-D) signatures of 5 classes (first row); eigenvectors corresponding to the largest eigenvalue (second row) and the second largest eigenvalue (third row) of ψ for corresponding signatures. These eigenvectors are basis functions of the m-D signatures.

and TNO. The measured data have been made available for the present study.

The UAVs considered for classification by the proposed technique are listed with their characteristics in Table 1. Different types of the UAVs are considered: two planes, a quadrocopter and three helicopters. For comparison, stationary rotating rotors with different number of blades as well as diverse species of birds are considered for classification. At least 30 s were recorded of each class. The data were recorded at open space with the distance to target less than 30 m. The aspect angle, distance and velocity were varying as within the real situation.

For classification we formulate two problems:

11-classes problem where each class corresponds to different model of the UAV, and the goal is to determine the correct type as well as the model.
5-classes problem where each class consists of the data from the same type of aerial object, and the goal is to determine only the type of the flying object.

The radar signal is divided onto a number of non-overlapping segments of fixed length, by processing these segments a decision about the class label is made. The length of one segment is set to 0.5 s. To compute the STFT we use a sliding Hamming window of length $M = 128$ samples = 4 ms with overlapping of $L = 90$ corresponding to $0.9 \times 4 = 3.6$ ms[1]. Finally, the features extracted for the two different sample rates are concatenated to one feature vector.

Examples of m-D signatures of the considered classes are illustrated in Fig. 3. The classes can be separated even visually. The features we extract are based on eigenvectors of the signature and the first two of them are also shown in Fig. 3.

[1]The value of L was chosen based on visual quality of the spectrogram and memory restrictions of PC.

B) Performance analysis

To classify the type of UAV, we will use the machine learning approach. All available segments are divided into training and testing sets without overlapping. The decision about class membership is made by a predefined system of rules. The process of defining the system of rules is called learning; it is performed on the training set. The number of correctly classified segments determines the probability of correct classification as ratio to the total number of segments from the testing set.

The $K = 10$ cross-validation technique is applied to obtain robust classification rates. The initial data under analysis are split into K subsets of the same length, and $K-1$ subsets are used as a training dataset, and the remaining one as a testing dataset. The cross-validation process is repeated $K-1$ times ($K-1$-folds) with each of the K subsets used as a testing dataset. The K results from the folds are averaged to evaluate a single estimation. The cross-validation is applied in such a way that training and testing sets contain data from different trials (experiments).

First, we want to study the influence of the feature extraction parameters on the classification result. Therefore, the number of eigenpairs in (12) was varied as $Z = 1,2,\ldots,14$ and the number of calculated Fourier coefficients in (11) was varied as $I = 1,2,\ldots,40$. Total number of 560 classification results were obtained using ten-fold cross-validation for all possible pairs of Z and I. Then, the classification rates were averaged for all values of Z and I, to show the dependence on these variables in Fig. 4. Analyzing the dependences, we conclude the following:

- With increasing the number of Fourier coefficients, SVM classifiers show increase in the performance;
- For Naive Bayes classifier, the performance reaches the pick with 16 Fourier coefficients, with larger number the performance degrades due to the "curse of dimensionality" phenomenon;

https://doi.org/10.1017/S1759078714000282 Published online by Cambridge University Press

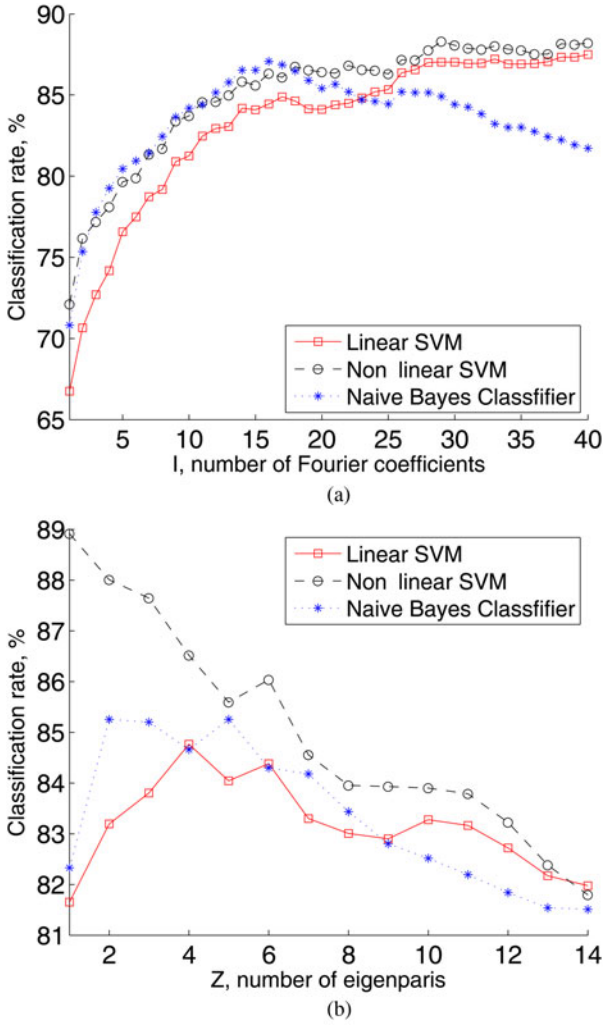

Fig. 4. Probability of correct classification for 11-classes problem depending on: (a) the number of Fourier coefficients in (11); (b) depending on the number of eigenpairs in (12).

- For non-linear classifiers, such as non-linear SVM, with increasing the number of eigenpairs, the performance degrades; the best result is obtained for only one eigenpair extracted.
- For linear classifiers, such as linear SVM and Naive Bayes classifier, the best performance is reached when several eigenpairs are extracted. Such for linear SVM, four eigenpairs provide the best performance, for Naive Bayes classifier five eigenpairs are selected.

According to the analysis we selected the following parameters:

- Non-linear SVM: $Z = 1$, $I = 29$;
- Linear SVM: $Z = 4$, $I = 33$;
- Naive Bayes classifier: $Z = 5$, $I = 16$;

Computed probabilities of correct classification for different classifiers are shown in Table 2. The results are shown for different sampling frequencies of the signal: 3.2, 32 kHz and when two of them are applied. The results in Table 2 allow us to conclude the following:

- For all classifiers the best results are obtained when two sampling frequencies are used;

Table 2. Probability of correct classification obtained for 11-classes problem using ten-fold cross validation.

Sampling type (kHz)	SVM linear (%)	SVM non-linear (%)	Naive Bayes (%)
3.2	73.79	74.75	69.22
32	86.3	86.14	88.28
32 and 3.2	89.86	92.3	88.42

- The benefit of processing the signal sampled at two sampling frequencies, compared to the best result out of one sampling frequency, is: SVM linear 3.56%; SVM non-linear 5.85%; Naive Bayes 0.14%;
- The best result is obtained with SVM nonlinear classifier: 92.3%.

Confusion matrix for non-linear SVM with applied ten-fold cross-validation is shown in Table 3 to estimate the intra class distribution of classification rates. It can be seen that all targets, except classes 1, 2 and 7, 8 are classified with probability of correct classification higher than 95%. The first two classes have more errors because blades are small and their m-D signatures are similar. The results for classes 5–8 show the capability to distinguish different number of rotors. The class #7, three stationary rotors, shows misclassification at level of 15% with class of four stationary rotors and helicopters class.

To show the flexibility of the proposed ATR scheme to classify different types of the UAVs, the following classes were removed from the training set: 1, 5, 6, 7, 9, 10. In this way for each type of the UAVs (plane, birds, stationery rotors, quadrocopter, and helicopter) only a single class is used for training. The removed classes are then used to test the system. The results of classification by linear SVM classifier are listed in the Table 4. The class of stationary rotating rotor, and the class of helicopters are classified correctly with 100%; the data from class 1 are classified correctly as a class of plane with probability of 86%. We can claim that proposed ATR scheme is robust to variations inside the class, and therefore with high probability, other UAVs with similar flying concept will be classified correctly.

For ATR system, it is important to reject an unknown target which class significantly differs from the ones used for training. To reject the unknown target a confidence threshold can be set. By confidence threshold, we mean a minimum

Table 3. Confusion matrix (in percentages) for linear SVM classifier, 11-classes problem.

Class	1	2	3	4	5	6	7	8	9	10	11
1	**70**	22	4	2	0	0	0	0	0	0	2
2	17	**79**	2	2	0	0	0	0	0	0	0
3	0	5	**95**	0	0	0	0	0	0	0	0
4	1	0	3	**96**	0	0	0	0	0	0	0
5	0	0	0	0	**100**	0	0	0	0	0	0
6	0	0	0	0	0	**100**	0	0	0	0	0
7	0	0	0	0	0	0	**85**	8	7	0	0
8	0	0	0	0	0	0	4	**96**	0	0	0
9	0	0	0	0	0	0	0	0	**99**	1	0
10	0	0	0	0	0	0	0	0	2	**98**	0
11	0	1	0	0	0	0	0	0	0	0	**99**

https://doi.org/10.1017/S1759078714000282 Published online by Cambridge University Press

Table 4. Classification of UAVs hidden from training procedure, 11-classes problem.

Class	P	B	Q	S	H
1	**85**	11	4	0	0
5	0	0	0	**100**	0
6	0	0	0	**100**	0
7	0	0	0	**100**	0
9	0	0	0	0	**100**
10	0	0	0	0	**100**

Table 5. Classification of the unseen for training classes, 5-classes problem.

Class	Unknown	B	Q	S	H
P	**83**	0	13	5	0
B	0	**100**	0	0	0
Q	16	0	**84**	0	0
S	9	0	0	**91**	0
H	0	0	0	0	**100**

value of the class conditional probability (posterior probability) for which the decision is assumed to be true, otherwise the target is marked as unknown. Even for non-probabilistic classifiers, such as SVM, it is possible to estimate the approximated posterior probability based on distances to the hyperplanes [18]. If we set the confidence threshold to 0.85 then with high probability targets from classes not used for training will be rejected. To demonstrate this Table 5 is shown. The following classes were removed from training set: [1, 2, 5, 6, 7, 9, 10]. As classes 1 and 2 are removed, the classifier has no data to train the class of planes, and these classes are assumed to be from class of unknown target. According to Table 3, 83% of the data of the plane's class is classified as unknown; also, 16% of data from quadrocopter's class and 9% of the class of stationary rotating rotor are misclassified as unknown target (Table 5).

For all experiments above we used half of a second of the observation time to classify the target. Next, we show what a performance can be achieved when shorter interval is used for decision making. The training set is constructed in the same manner as before (using 0.5 s as segment's duration); however, for training set, the features are extracted from shorter segments. This shows the robustness of the feature extraction procedure to the duration of the segment.

Figure 5 demonstrates the dependence of the classification rates on the dwell time for 11-classes problem. The following conclusions can be pointed out:

- Both SVM classifiers demonstrate stable result with dwell time longer than 0.25 s;
- Naive Bayes classifier provides a decrease of 4% with dwell time of 0.25 s;
- With dwell time shorter than 0.25 s, the performance drops significantly with decrease of the dwell time. At dwell time 0.05 s the following result is achieved: linear SVM 75%, non-linear SVM 82%, Naive Bayes classifier 65%.

Noise can corrupt the signal and degrade the classification performance. We will add white Gaussian noise to experiments from test dataset and examine the performance of the

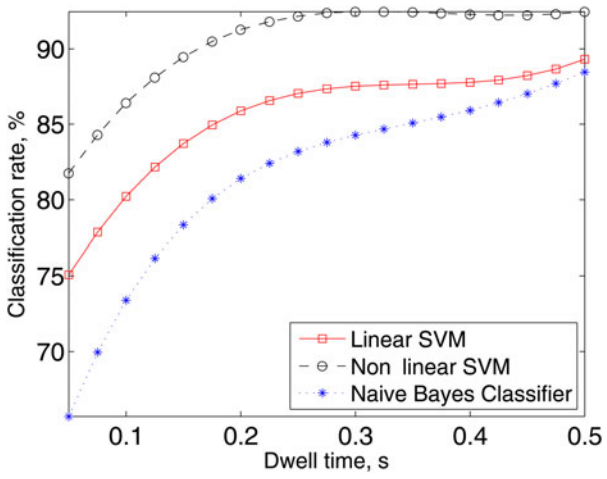

Fig. 5. Classification rate for 11-class problem depending on the dwell time.

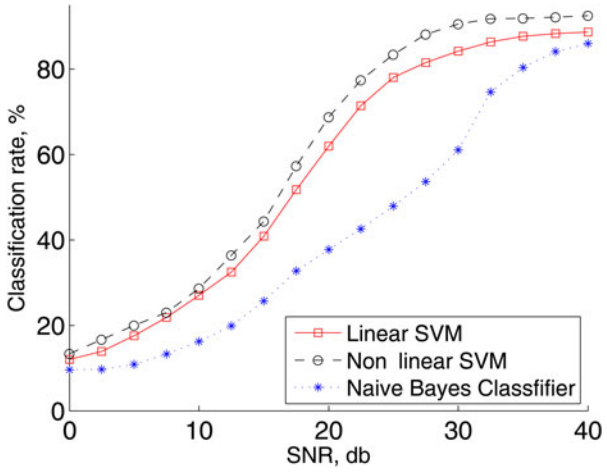

Fig. 6. Classification rate depending on SNR, 11-classes problem.

system. To do this, we assume that collected radar signal contains no noise and the power of the raw data will be used to calculate Signal to Noise Ratios (SNRs). Additive white Gaussian noise is generated as variable $\epsilon(n)$ in (2). Figure 6 demonstrates the dependence of classification rate on SNR, for 11-classes problem. We can conclude the following:

- The proposed approach together with SVM classifier demonstrates robustness to the SNR when it is higher than 30 dB;
- Performance drops to half with SNR = 18 dB, and reaches probability of random guess at 0 dB;
- Naive Bayes classifier together with the proposed approach is more sensitive to the SNR; drop to the half of the performance is obtained with 25 dB and than rapidly decreases.

V. MAIN CHALLENGES

The proposed ATR system applies eigendecomposition of the correlation matrix for feature extraction. This step is the most consuming of the overall system. For current computers it is not a problem; however for embedded systems it could be, for example in case of multiple target scenario. The

https://doi.org/10.1017/S1759078714000282 Published online by Cambridge University Press

eigendecomposition could be replaced with calculation of projection of the spectrogram onto a dictionary. Dictionary could be constructed only once during the training stage, it should contain eigenvectors extracted from the training data.

Another challenge is a robust alignment of the m-D signature. Proposed feature extraction algorithm requires m-D signature to be properly aligned. The current alignment method does not assume discontinues in the m-D signature (e.g. when a part of the signature is shadowed by another object.) For such scenarios, more robust alignment procedure is required.

Alignment procedure used in the system assumes that the highest reflectivity line in Doppler signature corresponds to main body of UAV. However, in some cases this assumption is not true, e.g. because of a special body construction or material. In this case, the alignment procedure will align the Doppler signature with respect to the highest reflectivity which could correspond to blades. Next, the track will be corrected by polynomial regression, and with high probability it will be associated correctly. Moreover, following feature extraction procedure does not require full compensation of the main body (to be at zero Doppler), any constant value will lead to the same features (because of amplitude spectrum's invariance to the spatial shift).

VI. CONCLUSIONS

A new automatic target recognition system has been proposed for classification of unmanned aerial targets by their m-D signatures. The preprocessing steps of the signature such as filtering and Doppler alignment have been discussed. New, robust features for target classification based on extraction of bases of the m-D signature have been introduced. The probability of correct classification of the order of 92% has been achieved. It has been shown that different models of the same type could be distinguished, helicopters with probability of 98%, stationary rotors near 95%, and planes with 74.5%. It was shown that system can identify unknown classes as well as classify models of UAVs excluded from the training procedure.

ACKNOWLEDGEMENTS

Pavlo Molchanov is supported by Graduate School in Electronics, Telecommunications, and Automation, Finland, by Foundation of Nokia Corporation, and by Arvoisa Henry Fordin Säätiön Grant number No. 201300176.

REFERENCES

[1] Toscano, M.: Unmanned aircraft systems roadmap to the future, in 7th North Dakota Research Corridor UAS Summit, May 2013, 569–572.

[2] Koolhoven, M.: Ratelband drone plane crash at Binnenhof. http://www.telegraaf.nl/binnenland/20876587/__Ratelband_laat_vliegtuigje_crashen__.html, September 2013.

[3] RT, German 'Pirates' stage mini-drone stunt at Merkel rally. http://rt.com/news/pirates-drone-stunt-merkel-953/, September 2013.

[4] Skolnik, M.: Introduction to Radar Systems, New York, McGraw-Hill, 1962.

[5] Clemente, C.; Balleri, A.; Woodbridge, K.; Soraghan, J.: Developments in target micro-doppler signatures analysis: radar imaging ultrasound and through-the-wall radar. EURASIP J. Adv. Signal Process., **2013** (1) (2013), 47.

[6] Chen, V.: The Micro-Doppler Effect in Radar, Artech House, London, 2011.

[7] de Wit, J.J.M.; Harmanny, R.I.A.; Prémel-Cabic, G.: Micro-Doppler analysis of small UAVs, in Radar Conf. (EuRAD), 2012 European, Amsterdam, The Netherlands, October 2012, 210–213.

[8] Bullard, B.; Dowdy, P.: Pulse doppler signature of a rotary-wing aircraft. Aerosp. Electron. Syst. Mag., IEEE, **6** (5) (1991), 28–30.

[9] Chen, V.; Ling, H.: Time-Frequency Transforms for Radar Imaging and Signal Analysis, Boston, MA, Artech House Radar Library, Artech House, 2002.

[10] Yoon, S.-H.; Kim, B.; Kim, Y.-S.: Helicopter classification using time-frequency analysis. Electron. Lett., **36** (22) (2000), 1871–1872.

[11] Cilliers, A.; Nel, W.A.J.: Helicopter parameter extraction using joint time-frequency and tomographic techniques, in 2008 Int. Conf. on Radar, Adelaide, SA, 2008, 598–603.

[12] Setlur, P.; Ahmad, F.; Amin, M.: Helicopter radar return analysis: estimation and blade number selection. Signal Process., **91** (2011), 1409–1424.

[13] Thayaparan, T.; Abrol, S.; Riseborough, E.; Stankovic, L.; Lamothe, D.; Duff, G.: Analysis of radar micro-Doppler signatures from experimental helicopter and human data. Radar, Sonar Navig., IET, **1** (2007), 289–299.

[14] Park, J.; Lim, H.; Myung, N.: Analysis of jet engine modulation effect with extended Hilbert-Huang transform. Electron. Lett., **49** (3) (2013), 215–216.

[15] Vaseghi, S.V.: Advanced Digital Signal Processing and Noise Reduction, Chichester, UK, John Wiley & Sons, 2006.

[16] Duda, R.O.; Hart, P.E.; Stork, D.G.: Pattern Classification, 2nd ed., New York, NY, Wiley, 2001.

[17] Cortes, C.; Vapnik, V.: Support-vector network. Mach. Learn., **20** (1995), 273–297.

[18] Wu, T.; Lin, C.; Weng, R.: Probability estimates for multi-class classification by pairwise coupling. J. Mach. Learn. Res., **5** (2003), 975–1005.

Pavlo Molchanov received the B.Sc. and M.Sc. degrees, with distinctions, in Electrical Engineering from National Aerospace University, Ukraine, in 2008 and 2010, respectively. He is currently working toward the Ph.D. degree in the Tampere University of Technology, Tampere, Finland. His research interests include radar signal processing, pattern classification, and spectrum estimation.

Ronny Harmanny received his B.Sc. in Electrical Engineering in 1997 from the Hanze University of Applied Sciences, and his M.Sc. in Computer Science in 2000 from the University of Twente. In the same year, he joined Thales Nederland B.V. as a radar system designer. He currently holds the position of Advanced Development Engineer at Thales' R&D lab in Delft, where he is involved in several innovative radar projects and studies.

https://doi.org/10.1017/S1759078714000282 Published online by Cambridge University Press

Jacco de Wit received the M.Sc. and Ph.D. degrees in Electrical Engineering from Delft University of Technology, in 2000 and 2005, respectively. Since 2005 he is employed at TNO, Department of Radar Technology, as radar systems engineer. His main research interests include advanced radar signal processing and innovative radar system concepts.

Karen Egiazarian received the M.Sc. degree in mathematics from Yerevan State University in 1981, the Ph.D. degree in physics and mathematics from Moscow State University, Moscow, Russia, in 1986, and the D.Tech. degree from the Tampere University of Technology (TUT), Tampere, Finland, in 1994. He has been Senior Researcher in the Department of Digital Signal Processing, Institute of Information Problems and Automation, National Academy of Sciences of Armenia. Since 1996, he has been an Assistant Professor in the Institute of Signal Processing, TUT, and from 1999 a Professor, leading the Computational Imaging Group. His research interests are in the areas of applied mathematics, image, and video processing.

Jaakko Astola received the Ph.D. degree in mathematics from Turku University, Finland, in 1978. From 1976 to 1977, he was in the Research Institute for Mathematical Sciences, Kyoto University, Japan. Between 1979 and 1987, he was in the Department of Information Technology, Lappeenranta University of Technology, Finland. In 1984, he was a Visiting Scientist at the Eindhoven University of Technology, The Netherlands. From 1987 to 1992, he was an Associate Professor in applied mathematics at Tampere University, Finland. Since 1993, he has been a Professor of signal processing at Tampere University of Technology. From 2000 to 2011, he was a head of the Academy of Finland Centre of Excellence in Signal Processing. His research interests include signal processing, coding theory, spectral techniques, and statistics.

https://doi.org/10.1017/S1759078714000282 Published online by Cambridge University Press